JCI The Journal of Clinical Investigation

RETRACTED

View retraction

Amendment history:
- Retraction (November 2020)
- Expression of Concern (September 2020)

Targeting NEK2 attenuates glioblastoma growth and radioresistance by destabilizing histone methyltransferase EZH2

Jia Wang, … , Maode Wang, Ichiro Nakano

J Clin Invest. 2017. https://doi.org/10.1172/JCI89092.

Research Article **Oncology** **Stem cells**

Accumulating evidence suggests that glioma stem cells (GSCs) are important therapeutic targets in glioblastoma (GBM). In this study, we identified NIMA-related kinase 2 (NEK2) as a functional binding protein of enhancer of zeste homolog 2 (EZH2) that plays a critical role in the posttranslational regulation of EZH2 protein in GSCs. NEK2 was among the most differentially expressed kinase-encoding genes in GSC-containing cultures (glioma spheres), and it was required for in vitro clonogenicity, in vivo tumor propagation, and radioresistance. Mechanistically, the formation of a protein complex comprising NEK2 and EZH2 in glioma spheres phosphorylated and then protected EZH2 from ubiquitination-dependent protein degradation in a NEK2 kinase activity–dependent manner. Clinically, NEK2 expression in patients with glioma was closely associated with EZH2 expression and correlated with a poor prognosis. NEK2 expression was also substantially elevated in recurrent tumors after therapeutic failure compared with primary untreated tumors in matched GBM patients. We designed a NEK2 kinase inhibitor, compound 3a (CMP3a), which efficiently attenuated GBM […]

Find the latest version:

https://jci.me/89092/pdf

Targeting NEK2 attenuates glioblastoma growth and radioresistance by destabilizing histone methyltransferase EZH2

Jia Wang,[1,2] Peng Cheng,[2,3] Marat S. Pavlyukov,[2,4] Hai Yu,[1,2] Zhuo Zhang,[2] Sung-Hak Kim,[5] Mutsuko Minata,[2] Ahmed Mohyeldin,[6] Wanfu Xie,[1] Dongquan Chen,[7] Violaine Goidts,[8] Brendan Frett,[9,10] Wenhao Hu,[11] Hongyu Li,[9] Yong Jae Shin,[12,13] Yeri Lee,[12] Do-Hyun Nam,[12,13,14] Harley I. Kornblum,[15,16,17] Maode Wang,[1] and Ichiro Nakano[2,18]

[1]Department of Neurosurgery, The First Affiliated Hospital of Xi'an Jiaotong University, Xi'an, Shaanxi, China. [2]Department of Neurosurgery, University of Alabama at Birmingham, Birmingham, Alabama, USA. [3]Department of Neurosurgery, The First Hospital, China Medical University, Shenyang, Liaoning, China. [4]Shemyakin-Ovchinnikov Institute of Bioorganic Chemistry, Moscow, Russia. [5]Department of Animal Science, College of Agriculture and Life Sciences, Chonnam National University, Gwangju, Republic of Korea. [6]Department of Neurological Surgery, James Comprehensive Cancer Center, The Ohio State University, Columbus, Ohio, USA. [7]Division of Preventive Medicine, University of Alabama at Birmingham, Birmingham, Alabama, USA. [8]Division of Molecular Genetics, German Cancer Research Center, Heidelberg, Germany. [9]Department of Pharmacology and Toxicology, University of Arizona, Tucson, Arizona, USA. [10]Synactix Pharmaceuticals Inc., Tucson, Arizona, USA. [11]Shanghai Engineering Research Center of Molecular Therapeutics and New Drug Development, East China Normal University, Shanghai, China. [12]Institute for Refractory Cancer Research, Samsung Medical Center, Seoul, Republic of Korea. [13]Department of Neurosurgery, Samsung Medical Center, Sungkyunkwan University School of Medicine, Seoul, Republic of Korea. [14]Department of Health Science and Technology, Samsung Advanced Institute for Health Science and Technology, Sungkyunkwan University, Seoul, Republic of Korea. [15]Departments of Psychiatry, [16]Pharmacology, and [17]Pediatrics, David Geffen School of Medicine, UCLA, Los Angeles, California, USA. [18]Comprehensive Cancer Center, University of Alabama at Birmingham, Birmingham, Alabama, USA.

Accumulating evidence suggests that glioma stem cells (GSCs) are important therapeutic targets in glioblastoma (GBM). In this study, we identified NIMA-related kinase 2 (NEK2) as a functional binding protein of enhancer of zeste homolog 2 (EZH2) that plays a critical role in the posttranslational regulation of EZH2 protein in GSCs. NEK2 was among the most differentially expressed kinase-encoding genes in GSC-containing cultures (glioma spheres), and it was required for in vitro clonogenicity, in vivo tumor propagation, and radioresistance. Mechanistically, the formation of a protein complex comprising NEK2 and EZH2 in glioma spheres phosphorylated and then protected EZH2 from ubiquitination-dependent protein degradation in a NEK2 kinase activity–dependent manner. Clinically, NEK2 expression in patients with glioma was closely associated with EZH2 expression and correlated with a poor prognosis. NEK2 expression was also substantially elevated in recurrent tumors after therapeutic failure compared with primary untreated tumors in matched GBM patients. We designed a NEK2 kinase inhibitor, compound 3a (CMP3a), which efficiently attenuated GBM growth in a mouse model and exhibited a synergistic effect with radiotherapy. These data demonstrate a key role for NEK2 in maintaining GSCs in GBM by stabilizing the EZH2 protein and introduce the small-molecule inhibitor CMP3a as a potential therapeutic agent for GBM.

Introduction

Glioblastoma (GBM) is the most prevalent and lethal primary brain tumor in adults, with a median overall survival of less than 2 years after diagnosis, even with maximal therapy (1, 2). Survival rates for patients with GBM are dismal, with 2-year survival rates ranging from 26% to 33% and 5-year survival rates below 5% (3, 4). The standard treatment for GBM includes maximal safe surgical resection, followed by radiotherapy and chemotherapy with temozolomide (TMZ) (2, 5, 6). However, life-threatening tumor recurrences are inevitable in the vast majority of patients given the best available treatments (4, 7). Recent studies have shown that, like some other malignant tumors, GBM exhibits a large range of phenotypic, molecular, and cellular heterogeneity, and a small subpopulation of tumor cells, termed glioma stem cells (GSCs), is responsible for tumorigenesis, treatment resistance, and subsequent tumor recurrence (8, 9). Therefore, it is critical to elucidate the molecular mechanisms underlying the maintenance of the characteristics of the GSC population and the resistance of these cells to radiotherapy or chemotherapy.

NIMA-related kinase 2 (NEK2) is a poorly characterized serine/threonine kinase that belongs to the NIMA-related kinase family (10). Recent studies suggest that during the mitotic phase of the cell cycle, NEK2 activation leads to the phosphorylation of centrosomal NEK2-associated protein 1 (C-NAP1), rootletin, and β-catenin (11). These proteins function to link paired centrosomes during interphase, and their subsequent phosphorylation results in their dissociation from the centrosome, promoting centrosome separation (12, 13). Other studies suggest that NEK2 transcription is increased in several cancer types and associated with poor survival rates (14, 15). In colorectal cancer, NEK2 expression is regulated by miR-128 (16), and in ovarian cancers, NEK2 overexpression promotes drug resistance through the regulation of the cell cycle and microtubules (17). Another study reported that NEK2 protein is associated with

Conflict of interest: The authors have declared that no conflict of interest exists.
Submitted: June 14, 2016; **Accepted:** June 8, 2017.
Reference information: *J Clin Invest*. https://doi.org/10.1172/JCI89092.

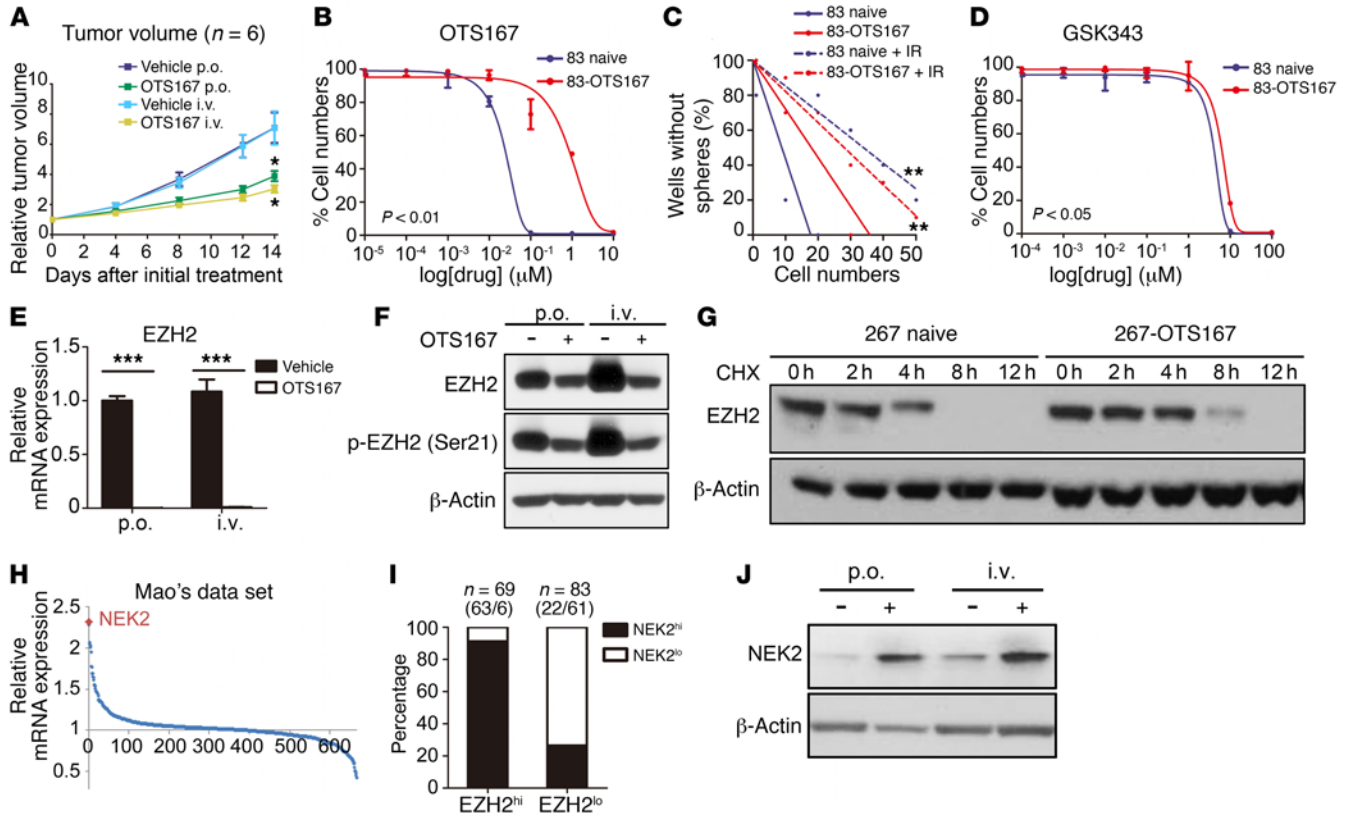


Figure 1. NEK2 plays an essential role in the posttranslational regulation of EZH2. (**A**) OTS167 treatment attenuated tumor growth in a U87 sub-Q xenograft mouse model ($n = 6$). *$P < 0.05$, by 1-way ANOVA. (**B**) Long-term OTS167 treatment induced a resistant population in 83 glioma spheres ($n = 6$). $P < 0.01$, by 1-way ANOVA. (**C**) An in vitro clonogenicity assay using limiting dilution neurosphere formation indicated that the OTS167-resistant population in 83 glioma spheres was more resistant to radiotherapy (IR) ($n = 10$). **$P < 0.01$, by ELDA. (**D**) An in vitro cell viability assay indicated that the OTS167-resistant population in 83 glioma spheres was still sensitive to the EZH2 inhibitor GSK343 ($n = 6$). $P > 0.05$, by 1-way ANOVA. (**E**) qRT-PCR showed that EZH2 expression was dramatically decreased by OTS167 treatment in a U87 tumor from a sub-Q xenograft mouse model ($n = 3$). ***$P < 0.001$, by 2-tailed t test. (**F**) Western blotting showed that EZH2 protein was only modestly affected by OTS167 treatment in a U87 tumor from a sub-Q xenograft mouse model. Replicate samples were run on parallel gels to obtain total EZH2 and phosphorylated EZH2 (p-EZH2) (Ser21) at the same time. (**G**) Western blotting for a CHX assay of 267 glioma spheres pretreated with OTS167 at the IC_{50} concentration (10 nM) for 4 weeks. (**H**) Genome-wide transcriptome microarray analysis (GSE67089) showed that NEK2 was the most upregulated kinase-encoding gene in glioma spheres. (**I**) NEK2 showed a strong association with EZH2 expression at the protein level in THPA database ($EZH2^{hi}$ samples, $n = 69$; $EZH2^{lo}$ samples, $n = 83$). (**J**) Western blotting indicated that NEK2 expression was increased in a U87 sub-Q xenograft mouse model after OTS167 treatment.

the phosphorylation of highly expressed cancer protein 1 (HEC1) at serine 165, thereby modulating chromosome segregation (18). Despite these findings, the physiological role of NEK2 and its molecular targets in GBM and cancer stem cells remain elusive.

Polycomb group (PcG) proteins are essential epigenetic regulators of somatic and cancer stem cells. They play a critical role in embryonic development and cell fate decisions (19). Furthermore, PcG proteins execute transcriptional repression in 2 multiprotein complexes, termed polycomb-repressive complexes 1 and 2 (PRC1 and PRC2). Enhancer of zeste homolog 2 (EZH2) is one of the core functional components in PRC2, and it functions as a lysine methyltransferase and catalyzes the trimethylation of histone H3 at lysine 27 (H3K27me3) (20). Recent studies have demonstrated that EZH2 expression is elevated in various human cancer types, including prostate cancer, breast cancer, and GBM, and it is closely associated with tumor malignancy and poor patient outcomes (21–23). We recently identified that EZH2 binds to and catalyzes the methylation of STAT3, thereby enhancing STAT3 activity in GSCs and regulating GSC self-renewal and survival (23). We also found that EZH2-mediated GSC maintenance and the radiation resistance of GSCs depend on maternal embryonic leucine zipper kinase (MELK) by its protein complex formation with the transcription factor FOXM1 (24). These studies led us to speculate that the MELK/EZH2/STAT3 signaling axis is a central regulator for GSC tumorigenicity in GBM.

In this study, we initially tested the efficacy of the MELK inhibitor OTS167 in a mouse intracranial model of human-derived glioma xenografts. OTS167 showed short-term efficacy by inhibiting GBM growth in vivo. However, GSC-containing cultures subsequently established resistance to MELK inhibition. Unexpectedly, these MELK-independent glioma spheres retained their EZH2 dependence, as both naive and MELK inhibitor–resistant glioma spheres from the same patients were equally sensitive to EZH2 inhibition. These data led us to identify the poorly studied serine/threonine kinase NEK2 as a protein-binding partner for EZH2, thereby promoting its stabilization in glioma spheres. As a result, in this study, we sought to focus on the characterization of NEK2 in GBM tumors and their oncogenic stem cells.

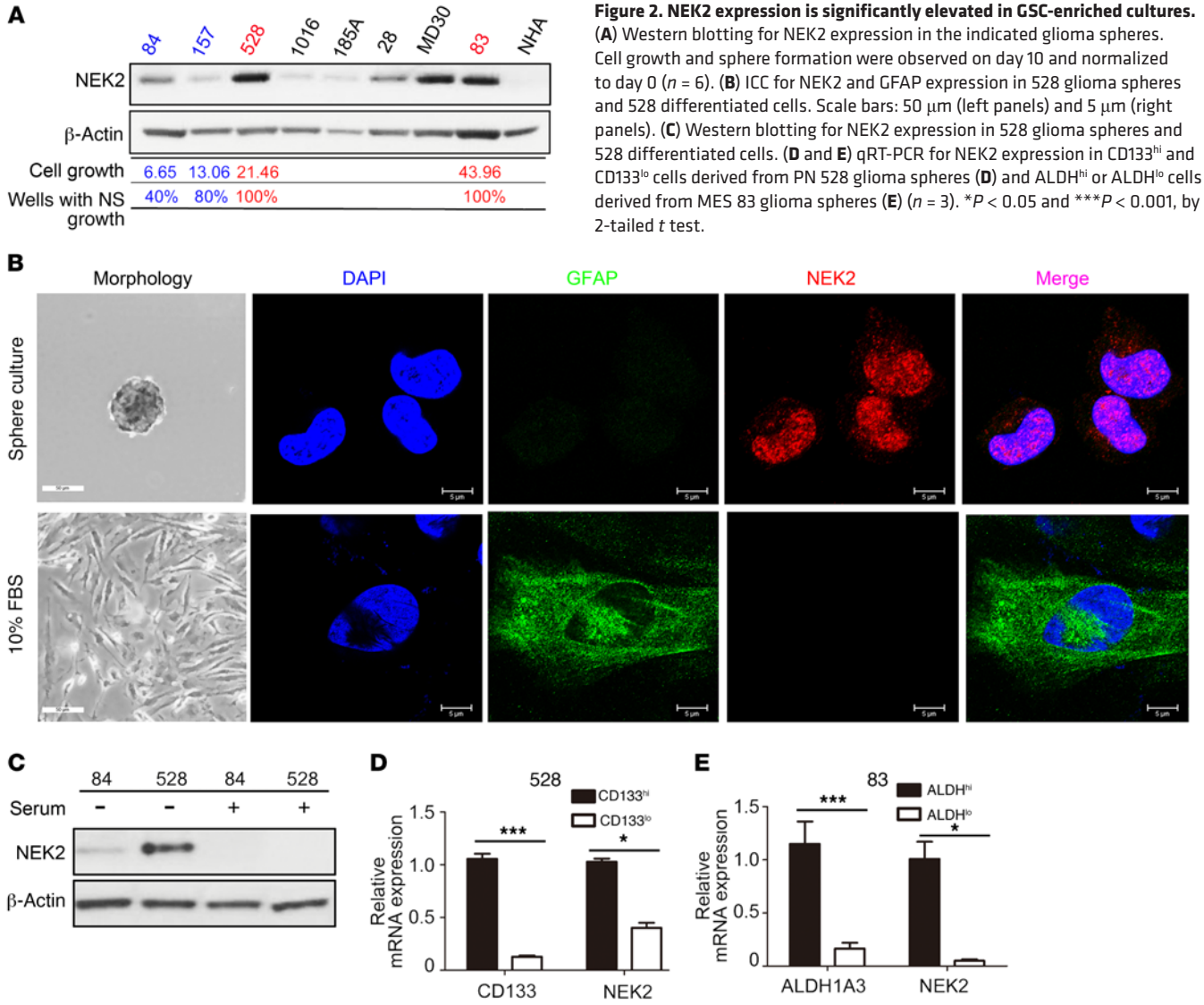


Figure 2. NEK2 expression is significantly elevated in GSC-enriched cultures. (**A**) Western blotting for NEK2 expression in the indicated glioma spheres. Cell growth and sphere formation were observed on day 10 and normalized to day 0 ($n = 6$). (**B**) ICC for NEK2 and GFAP expression in 528 glioma spheres and 528 differentiated cells. Scale bars: 50 μm (left panels) and 5 μm (right panels). (**C**) Western blotting for NEK2 expression in 528 glioma spheres and 528 differentiated cells. (**D** and **E**) qRT-PCR for NEK2 expression in $CD133^{hi}$ and $CD133^{lo}$ cells derived from PN 528 glioma spheres (**D**) and $ALDH^{hi}$ or $ALDH^{lo}$ cells derived from MES 83 glioma spheres (**E**) ($n = 3$). $^{*}P < 0.05$ and $^{***}P < 0.001$, by 2-tailed t test.

Results

NEK2 plays an essential role in the posttranslational regulation of EZH2. In a previous study, we demonstrated that the radioresistance of GBM tumors depends on MELK-mediated EZH2 signaling in GSCs (24). The MELK kinase inhibitor OTS167 is currently being tested in a phase I clinical trial for solid nonbrain cancers (https://clinicaltrials.gov/ct2/show/NCT01910545?term=OTS167&rank=1). To investigate the efficacy of OTS167 in GBM, we tested the compound on the commercially available GBM cell line U87 as well as previously characterized patient-derived glioma sphere lines ($n = 7$) (Supplemental Figure 1, A and B; supplemental material available online with this article; https://doi.org/10.1172/JCI89092DS1). In vitro OTS167 treatment attenuated U87 cell growth in a dose-dependent manner, with an IC_{50} of 15 nM (Supplemental Figure 1A). Like the results with U87 cells, we observed potent inhibitory effects of OTS167 on patient-derived glioma sphere lines (Supplemental Figure 1B). We then examined in vivo efficacy using U87-derived xenograft mouse tumor models with 2 different regimens: oral gavage at 10 mg/kg for 14 consecutive days and i.v. injection at 20 mg/kg every other day for 14 days. In both cases, OST167 treatment strongly inhibited tumor growth in the mice, resulting in decreased tumor burden, while not affecting their body weight (Figure 1A and Supplemental Figure 1C).

Recent evidence suggests that the rapid induction of resistance is a major limitation of various kinase inhibitors in cancer treatment, because the tumors reemerge with therapy-resistant properties. Therefore, we treated 4 patient-derived glioma sphere lines with OTS167 at the IC_{50} doses for up to 4 weeks to investigate the subsequent OTS167 treatment–mediated phenotypical changes. When the sensitivities to OTS167 were compared between these long-term–treated glioma spheres and their untreated counterparts, the pretreated spheres had gained OTS167 resistance (Figure 1B and Supplemental Figure 1, D–F), suggesting the establishment of MELK inhibitor resistance after long-term OTS167 treatment. These MELK inhibitor–resistant glioma spheres also showed resistance to radiation and TMZ (Figure 1C and Supplemental Figure 1G). In contrast to these results, the glioma spheres that received long-term OTS167 treatment retained sensitivity to EZH2 inhibition via GSK343 treatment (Figure 1D and Supplemental Figure 1, H–J). To validate the mechanism of this action, we harvested

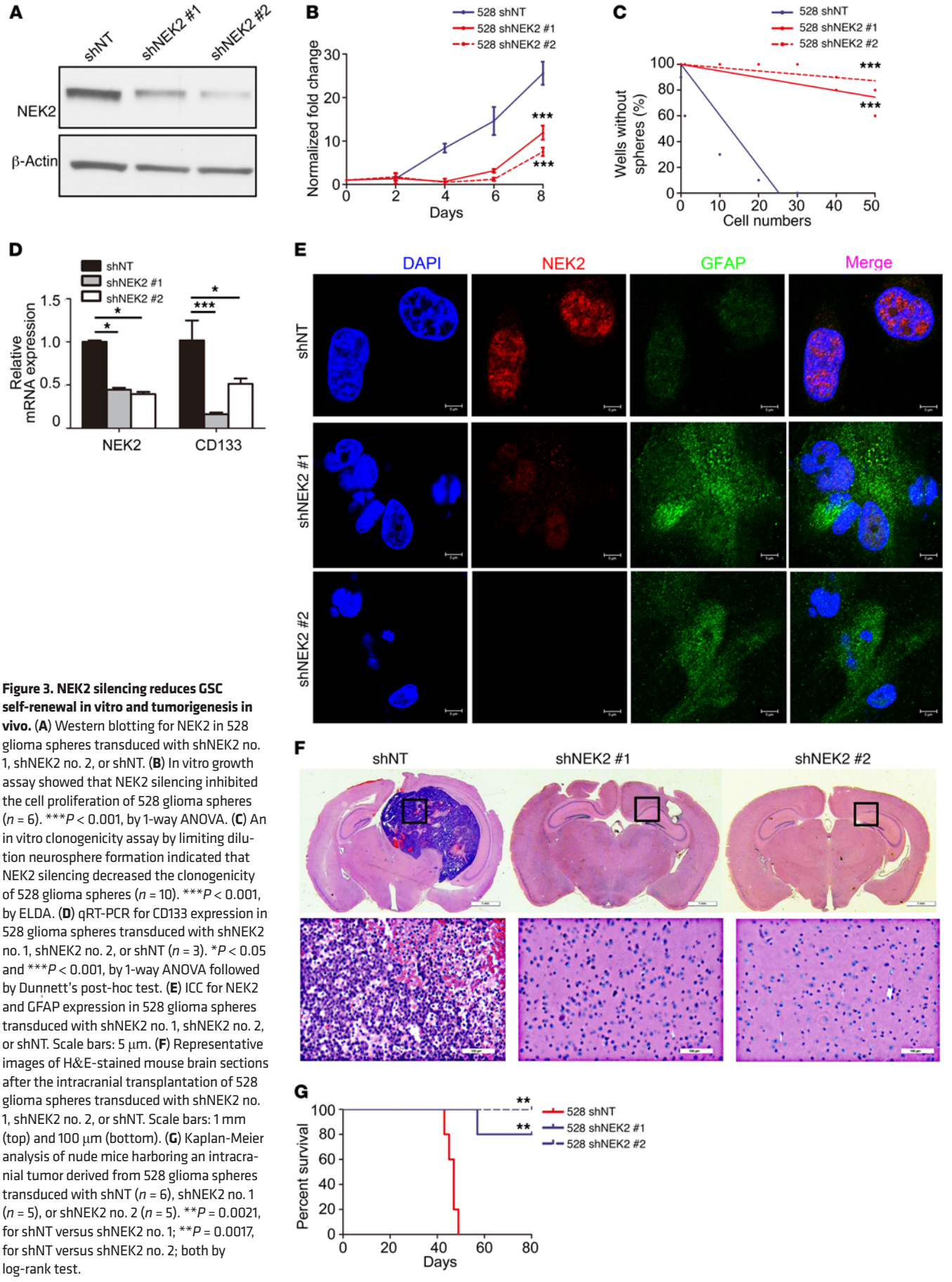


Figure 3. NEK2 silencing reduces GSC self-renewal in vitro and tumorigenesis in vivo. (**A**) Western blotting for NEK2 in 528 glioma spheres transduced with shNEK2 no. 1, shNEK2 no. 2, or shNT. (**B**) In vitro growth assay showed that NEK2 silencing inhibited the cell proliferation of 528 glioma spheres ($n = 6$). ***$P < 0.001$, by 1-way ANOVA. (**C**) An in vitro clonogenicity assay by limiting dilution neurosphere formation indicated that NEK2 silencing decreased the clonogenicity of 528 glioma spheres ($n = 10$). ***$P < 0.001$, by ELDA. (**D**) qRT-PCR for CD133 expression in 528 glioma spheres transduced with shNEK2 no. 1, shNEK2 no. 2, or shNT ($n = 3$). *$P < 0.05$ and ***$P < 0.001$, by 1-way ANOVA followed by Dunnett's post-hoc test. (**E**) ICC for NEK2 and GFAP expression in 528 glioma spheres transduced with shNEK2 no. 1, shNEK2 no. 2, or shNT. Scale bars: 5 μm. (**F**) Representative images of H&E-stained mouse brain sections after the intracranial transplantation of 528 glioma spheres transduced with shNEK2 no. 1, shNEK2 no. 2, or shNT. Scale bars: 1 mm (top) and 100 μm (bottom). (**G**) Kaplan-Meier analysis of nude mice harboring an intracranial tumor derived from 528 glioma spheres transduced with shNT ($n = 6$), shNEK2 no. 1 ($n = 5$), or shNEK2 no. 2 ($n = 5$). **$P = 0.0021$, for shNT versus shNEK2 no. 1; **$P = 0.0017$, for shNT versus shNEK2 no. 2; both by log-rank test.

U87-derived tumors treated with either OTS167 or vehicle (DMSO) for 2 weeks for analysis by quantitative real-time PCR (qRT-PCR) and Western blotting. As expected, EZH2 mRNA expression was substantially decreased by OTS167 treatment (Figure 1E). In contrast, EZH2 protein levels were only modestly affected by OTS167 treatment (Figure 1F). We then performed a protein degradation assay for EZH2 using 267 glioma spheres following 4 weeks of treatment with OTS167 at the IC_{50} dose (10 nM) or with DMSO with cycloheximide (CHX) to block protein synthesis. The EZH2 protein in 267 spheres treated with OTS167 for 4 weeks had a longer half-life than did that detected in the naive counterparts (Figure 1G). These data raised the possibility that some undetermined protein kinase may overcome the effects of OTS167 long-term treatment to sustain EZH2 activation, thereby retaining and even promoting GBM tumorigenesis and GSC stemness maintenance. To this end, we analyzed the microarray data from Mao's data set in the NCBI's Gene Expression Omnibus (GEO) database (GSE67089) (25) and found that NEK2 was the most upregulated kinase-encoding gene in glioma spheres compared with normal human astrocytes (NHAs) (Figure 1H). Furthermore, we searched The Human Protein Atlas (THPA), which contains the protein expression profiles of various human cancer types, including glioma, lung cancer, colorectal cancer, and breast cancer, to identify molecules that had expression profiles similar to those of EZH2. Expression of the serine/threonine kinase NEK2 had a strong association with EZH2 expression (Figure 1I and Supplemental Figure 1K). Additionally, a Pearson's correlation analysis was performed using The Cancer Genome Atlas (TCGA) database, and the results indicated that NEK2 was one of the most highly relevant kinase-encoding genes for EZH2 in GBM (Supplemental Table 1). Moreover, data analysis from the Ivy GBM database (http://glioblastoma.alleninstitute.org/) indicated that the expression of both NEK2 and EZH2 was highly enriched at the cellular tumor area and microvascular proliferation area of tumors compared with other regions within the tumor (Supplemental Figure 1, L and M). Interestingly, the results of Western blotting showed that NEK2 expression was substantially elevated in mouse GBM tumors after OTS167 treatment (Figure 1J). Taken together, these results suggest that NEK2 may play an essential role in the posttranslational regulation of EZH2 in GBM.

NEK2 expression is enriched in GSCs. Since NEK2 was the most upregulated kinase-encoding gene in glioma spheres compared with NHAs, we performed Western blotting to confirm this finding in glioma sphere models. The results revealed that NEK2 protein levels were elevated in glioma spheres from 13 patients compared with NEK2 levels in NHAs (Figure 2A and Supplemental Figure 2A). Although NEK2 expression varied within the glioma sphere lines, a correlation with faster growth and more clonogenic (neuro) sphere-forming cells was found in cell lines with higher NEK2 expression levels (Figure 2A and Supplemental Figure 2, B and C). We then compared NEK2 expression under 2 different culture conditions (serum-free and serum conditions). Immunocytochemistry (ICC) data showed that glioma spheres were highly immunoreactive to NEK2, with no detectable expression of the glial differentiation marker glial fibrillary acidic protein (GFAP), and this expression was reversed under serum conditions for 14 days (Figure 2B). Consistent with this finding, Western blotting showed that NEK2 expression was dramatically decreased in differentiated glioma spheres under differentiation conditions (Figure 2C). We further examined NEK2 expression in GSCs using an anti-CD133 antibody and an ALDEFLUOR assay for the enrichment of proneural (PN) GSCs and mesenchymal (MES) GSCs, respectively (25). NEK2 levels were elevated in GSCs enriched for the CD133 surface marker and the high-ALDH-activity population relative to matched negative tumor cells from 5 glioma sphere lines. (Figure 2, D and E, and Supplemental Figure 2, D–F). Taken together, these data indicate that NEK2 is preferentially expressed in GSCs.

NEK2 is functionally required for GSCs in vitro and in vivo. We then examined the pathophysiological role of NEK2 in glioma spheres. Two patient-derived glioma sphere lines (528 and 83) were transduced with either 1 of 5 lentiviral shRNA clones targeting NEK2 (shNEK2 D5–D9) or a nontargeting shRNA (shNT). The sequences of these shRNAs are described in Supplemental Table 2. Western blotting was used to validate the reduction of NEK2 expression after these shRNAs were transduced into the glioma spheres (Supplemental Figure 3A). On the basis of their knockdown efficiency, we then selected shNEK2 D6 and D7 (designated as shNEK2 no. 1 and shNEK2 no. 2) for a functional analysis of NEK2 in GSCs. Western blotting demonstrated that NEK2 protein expression was markedly decreased by shNEK2 no. 2 and, to a lesser extent, by shNEK2 no. 1 in 528 (Figure 3A) and 83 (Supplemental Figure 3A) glioma spheres. The in vitro cell growth kinetics of shNEK2-transduced 528 glioma spheres was diminished proportionally to the reduction of NEK2 by the 2 shRNA clones (Figure 3B). To assess the stem cell properties in the shNEK2-transduced glioma spheres, we performed a limiting dilution assay with 528 glioma spheres transduced with shNEK2 no. 1, shNEK2 no. 2, or shNT. Their clonal formation capability was substantially attenuated by NEK2 knockdown (Figure 3C and Supplemental Figure 3B). Similar results were obtained with the 83 glioma spheres (Supplemental Figure 3, B–D). In addition, NEK2-silenced 528 glioma spheres appeared to undergo differentiation, as evidenced by qRT-PCR data showing that CD133 expression was decreased after NEK2 was knocked down (Figure 3D). To confirm these results, we used another patient-derived glioma sphere sample (711 glioma spheres) infected with shNEK2 no. 2 or a control lentivirus, followed by qRT-PCR for stem cell–associated genes. Supplemental Figure 3E shows that the major stem cell genes (e.g., CD133, ABCG2, NANOG, OCT4, and SOX2) were downregulated by NEK2 knockdown in 711 glioma spheres. We also performed ICC on shNEK2-transfected glioma spheres with the glial differentiation marker GFAP. The result demonstrated that shNEK2-infected 528 glioma spheres had an increased GFAP immunoreactivity compared with that seen in the control cells (Figure 3E), indicating the possible differentiation of GSCs by NEK2 silencing.

Next, we investigated the effects of NEK2 knockdown on in vivo tumor formation. To this end, we used glioma sphere–derived mouse intracranial tumor models, as described previously (25). While the control mice with xenografts of shNT-transduced 528 glioma spheres rapidly formed lethal hypervascular GBM-like tumors within 50 days (with a median survival of 46.2 ± 2.28 days), most of the mice transplanted with shNEK2-transduced 528 glioma spheres failed to form tumors (Figure 3, F and G, and Supplemental Figure 3F), highlighting the potent antitumorigenic effect of NEK2 knockdown. We also obtained similar results in

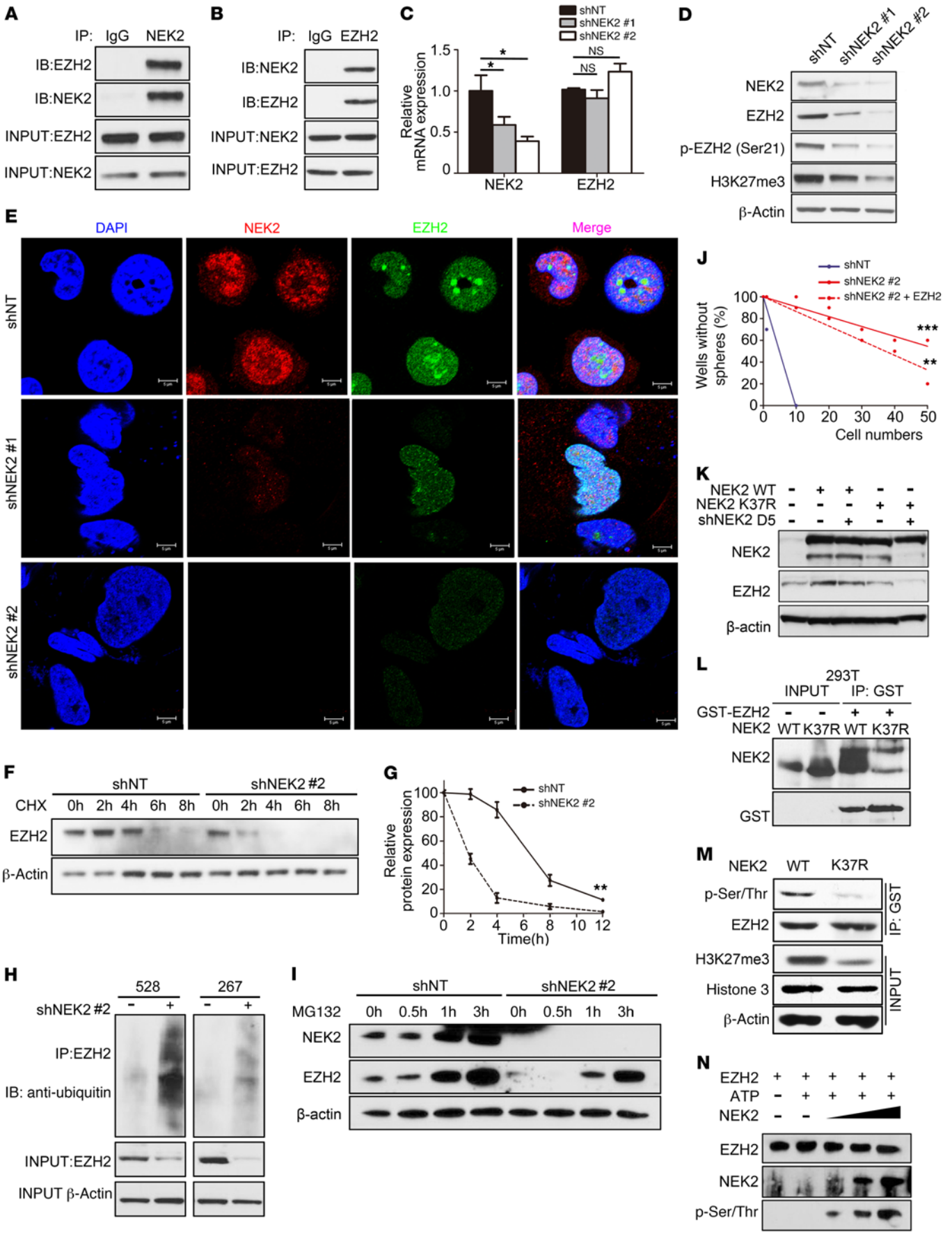

A
IP: IgG NEK2
IB:EZH2
IB:NEK2
INPUT:EZH2
INPUT:NEK2
B
IP: IgG EZH2
IB:NEK2
IB:EZH2
INPUT:NEK2
INPUT:EZH2
C
shNT
shNEK2 #1
shNEK2 #2
Relative mRNA expression
1.5
1.0
0.5
0
*
*
NS
NS
NEK2
EZH2
D
shNT
shNEK2 #1
shNEK2 #2
NEK2
EZH2
p-EZH2 (Ser21)
H3K27me3
β-Actin
E
DAPI
NEK2
EZH2
Merge
shNT
shNEK2 #1
shNEK2 #2
J
shNT
shNEK2 #2
shNEK2 #2 + EZH2
Wells without spheres (%)
100
80
60
40
20
0
0
10
20
30
40
50
Cell numbers
***
**
K
NEK2 WT - + + - -
NEK2 K37R - - - + +
shNEK2 D5 - - + - +
NEK2
EZH2
β-actin
L
293T
INPUT
IP: GST
GST-EZH2 - - + +
NEK2 WT K37R WT K37R
NEK2
GST
F
shNT
shNEK2 #2
CHX 0h 2h 4h 6h 8h 0h 2h 4h 6h 8h
EZH2
β-Actin
G
shNT
shNEK2 #2
Relative protein expression
100
80
60
40
20
0
0
2
4
6
8
10
12
Time(h)
**
M
NEK2 WT K37R
p-Ser/Thr
EZH2
IP: GST
H3K27me3
Histone 3
β-Actin
INPUT
H
528
267
shNEK2 #2 - + - +
IP:EZH2
IB: anti-ubiquitin
INPUT:EZH2
INPUT β-Actin
I
shNT
shNEK2 #2
MG132 0h 0.5h 1h 3h 0h 0.5h 1h 3h
NEK2
EZH2
β-actin
N
EZH2 + + + + +
ATP - + + + +
NEK2 - -
EZH2
NEK2
p-Ser/Thr

Figure 4. NEK2 signaling is mediated through the regulation of EZH2 protein stability in GSCs. (**A** and **B**) Immunoblotting (IB) for IP using a NEK2 antibody (**A**) or an EZH2 antibody (**B**) in 528 glioma spheres. IgG served as a control. (**C**) qRT-PCR for NEK2 and EZH2 expression in 528 glioma spheres transduced with shNEK2 no. 1, shNEK2 no. 2, or shNT ($n = 3$). $^*P < 0.05$ and $P > 0.05$ (NS), by 1-way ANOVA followed by Dunnett's post-hoc test. (**D**) Western blotting for NEK2, EZH2, p-EZH2 (Ser21), and H3K27me3 expression in 528 glioma spheres transduced with shNEK2 no. 1, shNEK2 no. 2, or shNT. (**E**) ICC for NEK2 and EZH2 in 528 glioma spheres transduced with shNEK2 no. 1, shNEK2 no. 2, or shNT. Scale bars: 5 μm. (**F** and **G**) Western blotting for EZH2 in CHX-treated 528 glioma spheres pretransduced with shNEK2 no. 2 or shNT (**F**). EZH2 had a shorter half-life in the presence of silenced NEK2 (**G**). $n = 3$. $^{**}P < 0.01$, by 1-way ANOVA. (**H**) The absence of NEK2 increased the ubiquitination of EZH2 in 528 and 267 glioma spheres. (**I**) Western blotting for EZH2 expression in MG132-treated 528 glioma spheres pretransduced with shNEK2 no. 2 or shNT. (**J**) An in vitro clonogenicity assay indicated that NEK2 silencing decreased the clonogenicity of 267 glioma spheres, which could be partially rescued by EZH2 overexpression ($n = 10$). $^{**}P < 0.01$ and $^{***}P < 0.001$, by ELDA. (**K**) Western blotting indicated that NEK2 silencing decreased EZH2 expression in 267 glioma spheres, which could be rescued by NEK2 WT but not K37R-mutant overexpression. (**L**) NEK2 WT or K37R-mutant proteins were subjected to a GST pull-down assay using GST-EZH2 and detected by immunoblotting. (**M**) Immunoblotting analysis indicated that EZH2 phosphorylation and H3K27me3 levels were decreased in K37R-overexpressed GBM-022 cells compared with WT-overexpressed cells. (**N**) An in vitro kinase phosphorylation assay showed that NEK2 phosphorylated EZH2 in a dose-dependent manner.

83 glioma spheres (Supplemental Figure 3, F–H). Taken together, these results indicate that NEK2 is required for GSC stemness maintenance and growth in vitro and in vivo.

NEK2 forms a protein complex with EZH2 to phosphorylate and then protect EZH2 from proteasome-dependent degradation in GSCs. Since there was an increase in NEK2 protein expression in response to EZH2 downregulation due to OTS167 treatment in glioma spheres, we hypothesized that NEK2 may contribute to the posttranslational regulation of EZH2. We performed IP experiments with an NEK2 antibody in glioma spheres. Immunoblotting analysis of the immunoprecipitated proteins indicated that NEK2 physically binded to EZH2 in 528 glioma spheres (Figure 4A). We confirmed this physical interaction between EZH2 and NEK2 by reciprocal IP using the same glioma spheres (Figure 4B). We further confirmed the results for this set of IP immunoblots using the 83 glioma spheres (Supplemental Figure 4, A and B).

Next, we investigated whether NEK2 silencing affected the temporal change of EZH2 expression in glioma spheres. qRT-PCR with shNEK2-transduced 528 glioma spheres showed no noticeable change in EZH2 mRNA expression compared with control cells (Figure 4C). In contrast, Western blotting results showed that EZH2 protein levels (both the total form and the phosphorylated active form) were strongly suppressed by NEK2 silencing in 528 glioma spheres (Figure 4D). The level of H3K27me3, a downstream target of EZH2, showed similar results (Figure 4D). Likewise, ICC showed a reduction of EZH2 protein by NEK2 knockdown in dissociated cells from 528 glioma spheres (Figure 4E). These results were confirmed in 83 glioma spheres (Supplemental Figure 4C). Furthermore, qRT-PCR showed that a set of EZH2 downstream target genes (24) were largely downregulated by NEK2 silencing in 528 glioma spheres (Supplemental Figure 4D). To elucidate the molecular mechanisms underlying the NEK2-mediated regulation of EZH2 protein levels in glioma spheres, we evaluated whether NEK2 silencing altered EZH2 protein expression by inhibiting de novo protein synthesis and/or promoting proteasome-mediated protein degradation. When 528 glioma spheres were pretreated with CHX, the EZH2 protein decayed more rapidly in the presence of shNEK2 transduction than in the presence of shNT transduction, indicating that NEK2 stabilized the EZH2 protein from degradation (Figure 4, F and G). Consistent with these results, ubiquitinated EZH2 levels were clearly increased in shNEK2 samples compared with levels in the shNT samples in the 2 glioma sphere lines (Figure 4H). Western blotting showed that pretreatment of the proteasome inhibitor MG132 caused the temporal accumulation of NEK2 and EZH2 protein in shNT-transduced 528 glioma spheres, whereas the initial shNEK2-mediated decrease in EZH2 protein levels was largely, if not completely, reversed by MG132 (Figure 4I and Supplemental Figure 4, E and F). Moreover, we obtained similar results with 83 glioma spheres (Supplemental Figure 4, G and H). Collectively, these data suggest that NEK2 is essential for protecting EHZ2 from proteasome-mediated protein degradation in glioma spheres.

Because we and others have reported that EZH2 is necessary for the maintenance of GSC phenotypes (23, 24), we further investigated whether exogenous EZH2 expression could rescue the effect of NEK2 silencing in glioma spheres. The attenuated proliferation and clonal sphere–formation ability resulting from NEK2 knockdown were both partially rescued by EZH2 overexpression (Figure 4J and Supplemental Figure 4, I and J). Furthermore, a wound-healing assay showed that 267 cell motility was decreased by NEK2 silencing and could be rescued by exogenous EZH2 expression (Supplemental Figure 4K). Altogether, NEK2 signaling in glioma spheres is at least partially mediated by the regulation of EZH2 protein stability.

To clarify whether the silencing of NEK2 altered EZH2 as a result of the loss of NEK2 protein or loss of NEK2 kinase activity, we designed overexpression vectors for NEK2 WT and the K37R mutant, which is a well-known major catalytically inactive mutation of NEK2 (26). We transfected these vectors into 267 glioma spheres, and the results demonstrated that shNEK2 decreased EZH2 expression and that this effect was rescued by the NEK2 WT overexpression vector but not by the K37R-mutant vector (Figure 4K). Additionally, the NEK2 WT and K37R proteins from 293T cells were subjected to a GST pull-down assay using GST-EZH2 and analyzed by immunoblotting using an anti-NEK2 antibody. The results showed that NEK2 WT protein could be strongly detected in the GST-EZH2 pull-down samples, while the K37R mutant showed a very limited association with EZH2 protein (Figure 4L). Similar results were observed in the GBM-022 cell line (Supplemental Figure 4, L and M). Furthermore, we used three 3′-UTR-shNEK2 lentiviral clones (shNEK2 D5, shNEK2 09, and shNEK2 48) to block NEK2 expression in 267 glioma spheres, and the NEK2-knockdown–induced attenuated proliferation could be rescued by exogenous NEK2 WT overexpression but not by the K37R mutant (Supplemental Figure 4, N–P). Moreover, GST-EZH2 was immunoprecipitated with anti-GST antibodies from a cell lysate of GBM-022 that was overexpressed with GST-EZH2 and either NEK2-WT or the K37R-mutant vector. Immunoblot analysis indicated that both EZH2 phosphorylation and H3K27me3 were dramatically decreased in the K37R-overexpressed GBM cells com-

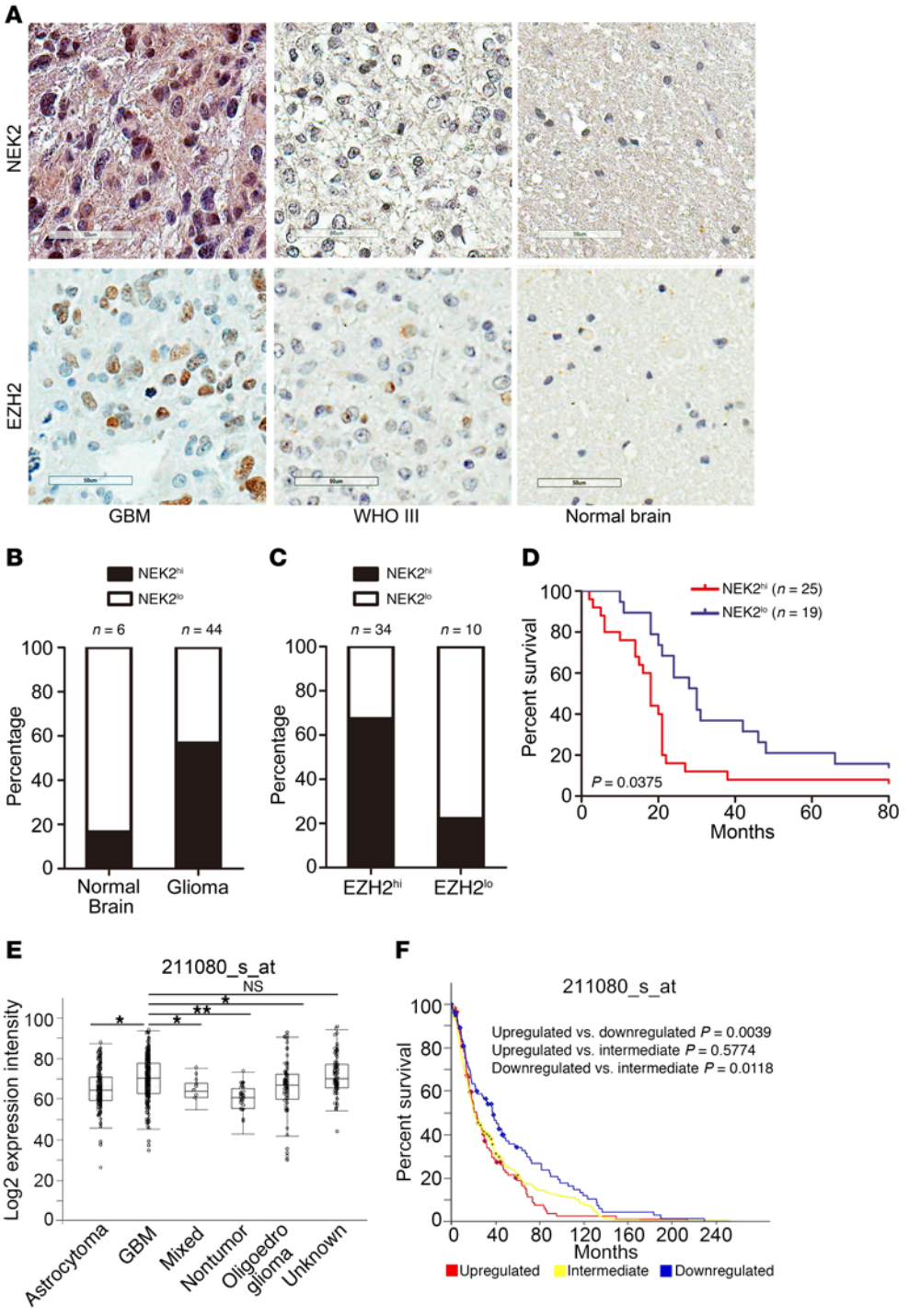


Figure 5. NEK2 is a clinically relevant molecular target in GBM. (**A**) Representative IHC images of NEK2 and EZH2 in glioma and nontumor brain samples. (**B**) An analysis of NEK2 in glioma (n = 44) and nontumor brain samples (n = 6) showed that NEK2 was highly expressed in glioma samples. (**C**) NEK2 expression in EZH2^{hi} (n = 34) and EZH2^{lo} (n = 10) glioma samples. Scale bars: 50 μm. (**D**) Kaplan-Meier analysis was performed to evaluate the correlation between NEK2 expression and the survival of 44 glioma patients. P = 0.0375, by log-rank test. (**E**) An analysis of the REMBRANDT data indicated that NEK2 expression was elevated in GBM samples. *P < 0.05 and **P < 0.01, and P > 0.05 (NS), by 1-way ANOVA followed by Dunnett's post-hoc test (probe set: 211080_s_at) (n = 541). (**F**) An analysis of the REMBRANDT data indicated an inverted correlation between NEK2 expression and the post-surgical survival of glioma patients. n = 117 for the NEK2-upregulated group, n = 314 for the NEK2-intermediate group, n = 110 for the NEK2-downregulated group (probe set: 211080_s_at). P values were determined by log-rank test.

pared with that observed in the WT-overexpressed cells (Figure 4M). Last, we performed an in vitro kinase phosphorylation assay to explore the phosphorylation effects of NEK2 on EZH2 protein. The results indicated that the cell-free phosphorylation of EZH2 was increased by NEK2 in a dose-dependent manner (Figure 4N). All together, these results indicate that NEK2 regulates the post-translational modification of EZH2 via NEK2 kinase activity.

NEK2 is highly expressed in glioma and is associated with a poor prognosis in glioma patients. Given the results from these experiments, we sought to determine whether NEK2 was a druggable target molecule in GBM. To address this question, we first examined NEK2 and EZH2 protein expression in 44 tumor tissue samples from patients with varying grades of glioma and 9 adjacent normal brain tissue samples using IHC. We detected high NEK2 expression levels in the cytoplasm and nuclei of some glioma tissues, and EZH2 was preferentially present in the nuclei of malignant glioma tissues (Figure 5A). We then used German IHC scores (GIS) to quantify the expression levels of NEK2 and EZH2 in each sample. NEK2 was highly expressed in approximately half of the glioma samples (25 of 44) but not in the majority of normal brain tissues (1 of 6 samples) (Figure 5B). At the same time, a trend indicated that gliomas with higher NEK2 expression also had higher EZH2 expression (23 of 34 samples) (Figure 5C).

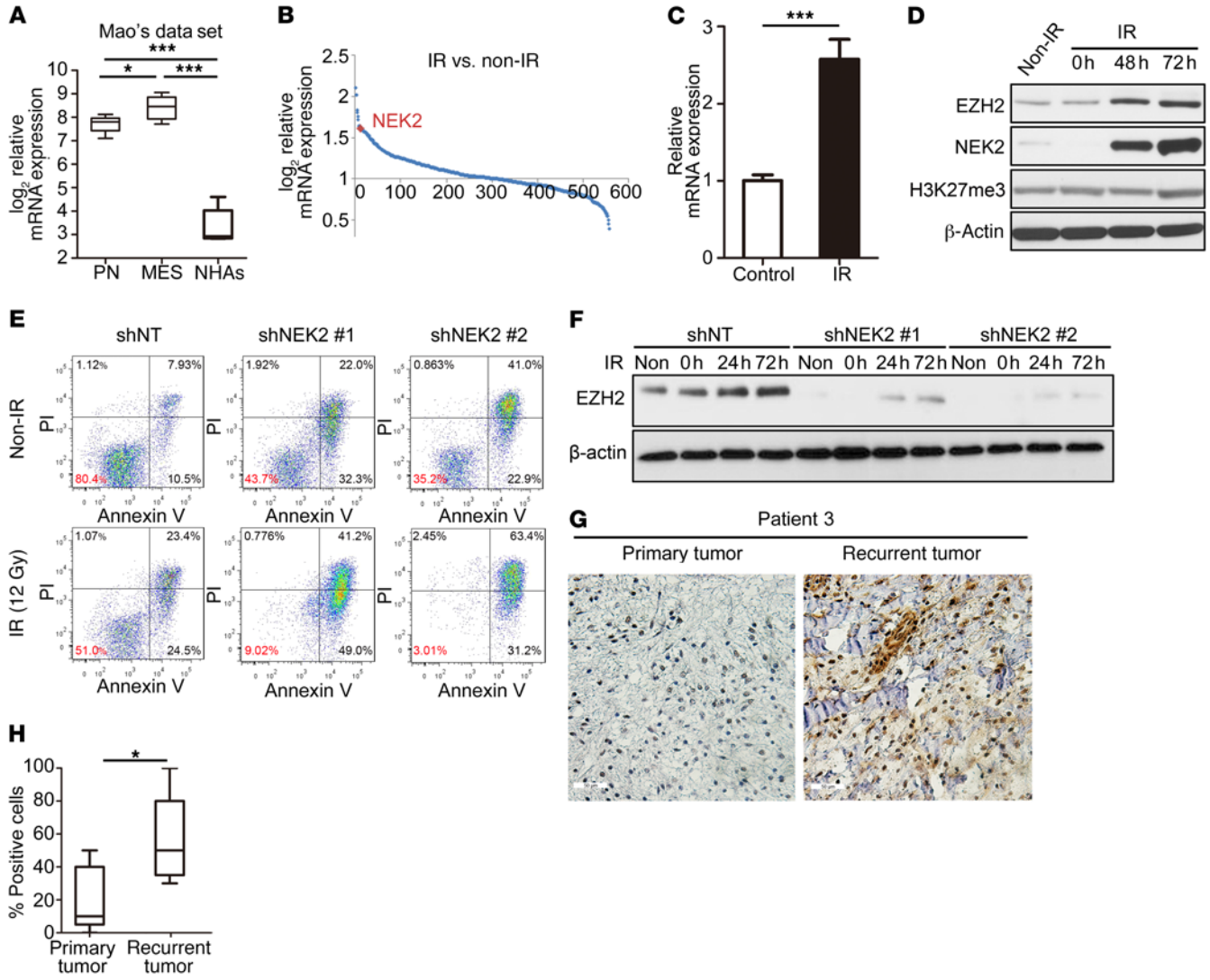


Figure 6. NEK2 promotes radioresistance in glioma spheres by maintaining EZH2 protein stability. (**A**) mRNA expression analysis (GSE67089) showed that NEK2 was highly enriched in glioma spheres compared with normal astrocytes. *$P < 0.05$ and ***$P < 0.001$, by 1-way ANOVA followed by Dunnett's post-hoc test. $n = 6$ for PN, $n = 3$ for MES and $n = 1$ for NHAs. 3 or more replicates were performed at the same time. (**B**) Genome-wide transcriptome microarray analysis showed that NEK2 was one of the most upregulated kinase-encoding genes in post-radiation glioma spheres (12 Gy) compared with naive glioma spheres. (**C**) qRT-PCR for NEK2 in post-radiation 528 glioma spheres (12 Gy) compared with naive 528 glioma spheres ($n = 3$). ***$P < 0.001$, by 2-tailed t test. (**D**) Western blotting for NEK2 and EZH2 in 528 glioma spheres treated with radiation (12 Gy) compared with naive 528 glioma spheres. (**E** and **F**) Flow cytometric analysis for apoptosis (**E**) and Western blotting for NEK2 and EZH2 expression (**F**) in 528 glioma spheres pretransduced with shNEK2 no. 1, shNEK2 no. 2 or, shNT and then treated with or without (Non) radiation (12 Gy). (**G**) Representative IHC images for NEK2 expression in primary untreated tumors and post-radiation recurrent tumors from matched GBM patients. (**H**) Percentage of NEK2 positive-stained cells in primary untreated tumors and post-radiation recurrent tumors from matched GBM patients ($n = 5$). *$P < 0.05$, by 2-tailed t test.

Furthermore, the survival period was significantly longer in the NEK-2^{lo} group than in the NEK2^{hi} group (Figure 5D). We observed the same results from an independent validation cohort including 56 patients' samples obtained through collaboration with the Department of Neurosurgery, The First Affiliated Hospital of Xi'an Jiaotong University (Supplemental Figure 5A). Additionally, we found that NEK2 and EZH2 expression levels were elevated and highly correlated in 4 subtypes of GBM in TCGA database (Supplemental Figure 5, B and C). Moreover, data from the REMBRANDT database (https://gdoc.georgetown.edu/gdoc/workflows/index) also demonstrated that NEK2 expression in GBM is significantly higher than that in nontumor and other lower-grade glioma groups (Figure 5E). Regarding the correlation of NEK2 expression with post-surgical patient outcomes, patients with higher NEK2 expression levels demonstrated significantly shorter survival periods than did those with intermediate or low expression levels (Figure 5F). In addition, another probe for NEK2 in the REMBRANDT database yielded consistent results (Supplemental Figure 5, D and E). These data indicate that NEK2 is likely a clinically relevant molecular target in GBM.

NEK2 promotes radioresistance in GSCs. We recently reported that EZH2 promotes radioresistance in GSCs (24). Therefore, we hypothesized that NEK2 may contribute to GSC radioresistance, thereby leading to tumor recurrence after therapeutic failure. In fact, NEK2 expression was highly enriched in MES GSCs, which

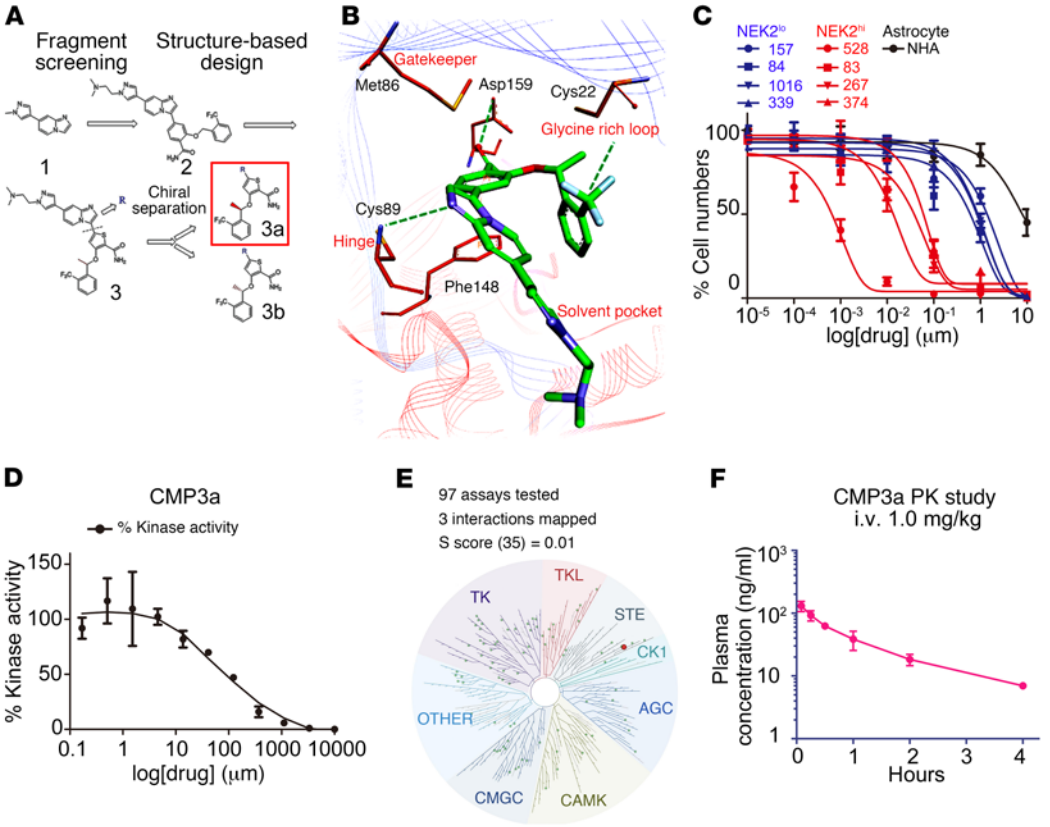


Figure 7. The NEK2 inhibitor CMP3a attenuates tumor growth and increases radiosensitivity in GBM. (**A**) General methods for the development of CMP3a. (**B**) Chemical structure of CMP3a. (**C**) In vitro cell viability assay for CMP3a with the NEK2^{hi} glioma spheres group (83, 267, 374, and 528) compared with the NEK2^{lo} glioma spheres group (84, 1016, 339, and 157) and NHAs (n = 6). $P < 0.05$, by 1-way ANOVA. (**D**) Relative kinase activity of NEK2 incubated with varying doses of CMP3a, determined by a cell-free in vitro kinase-binding assay (n = 3; IC_{50} = 82.74 nM). (**E**) CMP3a was screened at 15 nM against 97 kinases representing all kinase clusters using KINOMEscan. S score, KINOMEscan selectivity score (targets exhibiting less than 35% remaining activity). (**F**) PK analysis for CMP3a with 1.0 mg/kg i.v. injection in Wistar rats (n = 5). (**G**) Kaplan-Meier analysis for mice intracranially transplanted with 374 glioma spheres followed by a 10-day continuous treatment with different does of CMP3a or vehicle via tail vein injection (n = 6). P values were determined by log-rank test. (**H**) IP was performed with a NEK2 antibody or IgG in 528 glioma spheres, with or without CMP3a treatment. Immunoblotting was used to measure EZH2 expression. (**I**) Western blotting for EZH2 expression in CHX-treated 267 glioma spheres pretreated with CMP3a or DMSO. (**J**) An in vitro clonogenicity assay indicated that the combination of CMP3a with radiation (12 Gy) decreased the clonogenicity of 528 glioma spheres (n = 10). $^{**}P < 0.01$ and $^{***}P < 0.001$, by ELDA. (**K**) Chou-Talalay analysis showed a CI of radiation treatment and CMP3a, indicating that CMP3a had a synergistic effect with radiation. Fa, fraction affected.

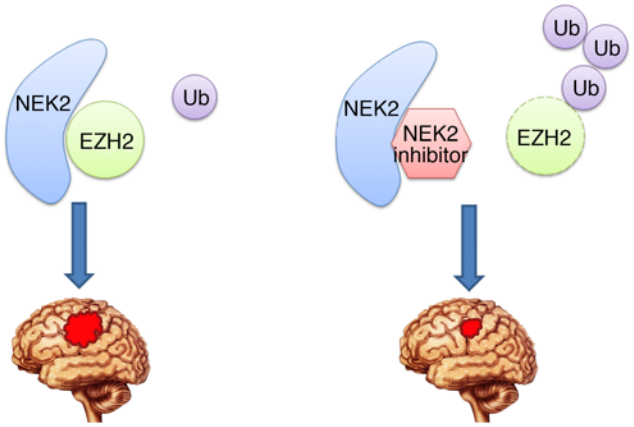


Figure 8. CMP3a inhibits proliferation and tumorigenicity in GSCs through interrupting EZH2-NEK2 interaction then results in a proteasomal degradation of the EZH2. Ub, ubiquitin.

were closely associated with the post-radiation recurrence of GBM (Figure 6A). A transcriptome microarray analysis focused on the 668 kinase–encoding genes in 2 glioma sphere samples with either a PN signature (AC17 glioma spheres) or a MES signature (83 glioma spheres) demonstrated that NEK2 was among the top 13 genes that were upregulated after 12-Gy radiation (Figure 6B). Both the qRT-PCR and Western blotting results indicated that NEK2 and EZH2 were similarly elevated in the 528 glioma spheres after radiation with 12 Gy (Figure 6, C and D). Similar results were observed with 83 glioma spheres (Supplemental Figure 6A). We then performed flow cytometry for apoptosis with an annexin V (AV) antibody and propidium iodide (PI) using shNEK2-transduced 528 glioma spheres, with or without radiation treatment (12 Gy). The proportions of cells undergoing early (AV^+, PI^-) and late (AV^+, PI^+) apoptosis were both dramatically increased after radiation when combined with NEK2 knockdown compared with radiation alone (Figure 6E). Along with this post-radiation increase in apoptosis via NEK2 knockdown, the post-radiation increase in EZH2 was largely, if not completely, eliminated by NEK2 knockdown in 528 glioma spheres (Figure 6F). Taken together, these data suggest that NEK2 promotes GSC radioresistance through the regulation of EZH2.

To investigate whether these results were clinically relevant, we collected 5 matched GBM tissues from the initial surgery for untreated tumors and from the second surgery after treatment failure with radiation and TMZ chemotherapy for NEK2 IHC analysis. Although the staining intensities for NEK2 varied among the GBM tissues from the initial surgeries, we observed an overall trend of increased NEK2 expression in recurrent tumors compared with naive tumor sections (4 of 5) (Figure 6G and Supplemental Figure 6, B and C). Similarly, the proportions of NEK2-positive tumor cells were generally increased in recurrent tumors compared with the matched primary tumors (Figure 6H). Collectively, NEK2 is upregulated in post-radiation GBM tissues and GSC-containing cultures, indicating that NEK2 may play an important role in the development of their radioresistance.

Development of a NEK2 inhibitor for GBM therapy. In an effort to develop NEK2-targeted cancer therapeutics, we sought to design clinically applicable small molecules that selectively inhibited NEK2 kinase activity in GSCs. To this end, we established a NEK2 computational binding model and a focused kinase inhibitor fragment library (300 compounds) to identify NEK2-selective inhibitors. An initial screening of this 300-compound kinase fragment library identified fragment 1 as having activity against NEK2 (IC_{50} = 20 μM). Using a computer-based drug discovery methodology with fragment 1, we designed and synthesized compound 2, which showed improved binding to the NEK2 active site according to the computational modeling (Figure 7A). Compound 2 indeed showed improved activity in the NEK2 enzymatic assay, with an IC_{50} of 0.1 μM. The introduction of a methyl group to the benzylic position and the replacement of the phenyl linker with a thiophene in compound 2 produced compound 3, which showed a 3-fold improvement in activity (IC_{50} = 0.03 μM). Compound 3 was a mixture of 2 enantiomers, and the pure single isomer 3a from the chiral separation was approximately 2-fold more potent (IC_{50} = 0.015 μM) than the racemic mixture 3, while the IC_{50} of the other isomer 3b was greater than 0.2 μM. The enantiopure single isomer 3a or 3b could be obtained from the commercially available R or S 1-(2-(trifluoromethyl)phenyl) ethanol (Figure 7A). Therefore, we selected compound 3a (hereafter designated CMP3a) as the lead candidate for GBM therapy (Figure 7B). The procedure for CMP3a synthesis is described in Supplemental Figure 7 and in the Supplemental Methods. To characterize the efficacy of this NEK2 inhibitor, we investigated the IC_{50} of CMP3a in different patient-derived glioma sphere samples. As expected, in vitro sensitivities of the glioma sphere cells to CMP3a were correlated with their NEK2 expression levels, while NHAs were markedly resistant to CMP3a (Figure 7C). A cell-free kinase-binding assay showed that NEK2 kinase activity was strongly inhibited by CMP3a at doses from 10 to 100 nM (IC_{50} = 82.74 nM), which were quite similar to the IC_{50} doses from our in vitro cytotoxicity assay (Figure 7D). To assess the specificity, CMP3a was screened at a concentration of 15 nM against 97 kinases representing all kinase clusters (KINOMEscan; https://www.discoverx.com/technologies-platforms/competitive-binding-technology/kinomescan-technology-platform). Only 3 kinases (YSK4, FLT3-ITDD835V, and FLT3-ITDF691L) showed greater than 65% inhibition. Therefore, CMP3a was relatively selective for NEK2 inhibition (Figure 7E and Supplemental Figure 8A). The pharmacokinetic (PK) profile of CMP3a was characterized in Wistar rats via a contract with Pharmacon. Using an i.v. dose of 1 mg/kg, CMP3a demonstrated the following PK properties: the elimination half-life ($t_{1/2}$) was 1.4 h; the clearance (CL) was 7,304 ml/h/kg; the volume of distribution (VOD) was 14,872 ml/kg; and the AUC was 130 mg/h/kg. Although the AUC was relatively low, most of the drug was probably distributed in the tissues, given the high VOD (Figure 7F). We then selected 2 HEC1/NEK2 inhibitors (INH1 and INH6) and 1 PLK1/NEK2 inhibitor (Ro3280) to compare the potential efficiency of CMP3a in attenuating tumor cell growth (Supplemental Figure 8, B–D). The in vitro data indicated that CMP3a attenuated glioma sphere cell growth more efficiently than did other inhibitors in 2 different glioma spheres (Supplemental Figure 8, E and F). Additionally, a cell-free kinase-binding assay indicated that CMP3a more efficiently inhibited NEK2 kinase activity than did the other 3 inhibitors (Supplemental Figure 8G). Next, we investigated the effect of CMP3a on in vivo tumor initiation and propagation using GSC-derived mouse intra-

cranial tumor models. CMP3a treatment was initiated 7 days after the xenotransplantation of 267 or 374 glioma spheres. The treatment was continued for 10 days via tail vein injection at a dose of 10 or 20 mg/kg/day. As expected, we observed decreased in vivo tumor growth and prolonged overall survival in the CMP3a-treated group compared with the vehicle-treated group (Figure 7G and Supplemental Figure 8, H and I). To determine whether CMP3a elicits any off-target effects, we performed IHC and observed a dramatic decrease of EZH2 in the tumors from a CMP3a-treated xenograft mouse model compared with EZH2 levels in the control group tumors (Supplemental Figure 8J).

Since NEK2 silencing decreased EZH2 expression by destabilizing the EZH2 protein, we treated glioma spheres with different concentrations of CMP3a for 48 hours. Western blotting indicated that EZH2 and H3K27me3 expression levels were reduced in a dose-dependent manner with NEK2 inhibition (Supplemental Figure 8K). We then purified the protein from the 528 glioma spheres treated with or without CMP3a (0.5 μM and 5 μM) for 2 hours, followed by IP with an NEK2 antibody. Immunoblot analysis showed that CMP3a treatment resulted in the blockage of NEK2-EZH2 complex formation (Figure 7H). Additionally, a CHX assay showed that the half-life of EZH2 protein was decreased in the glioma spheres after 24 hours of CMP3a treatment, a result similar to that seen with shNEK2 (Figure 7I).

As NEK2 has been shown to be a mitotic kinase, promoting tumor cell proliferation mainly through centrosome separation and bipolar spindle formation at the centrosome (15), we sought to clarify whether the function of NEK2 in GSCs mainly depends on the regulation of mitotic progression. ICC was performed, and acetylated α-tubulin was used to label the microtubes and centrosomes. We observed with a confocal microscope that NEK2 protein was still localized to the centrosomes after CMP3a treatment (Supplemental Figure 8L) and that glioma sphere mitosis was not largely affected by CMP3a treatment (Supplemental Figure 8M). Additionally, flow cytometry showed that NEK2 expression in DMSO- or CMP3a-treated glioma spheres was comparable in all phases of the cell cycle, including the mitotic phase (Supplemental Figure 8N). Furthermore, flow cytometry demonstrated that NEK2 inhibition by CMP3a did not cause any noticeable changes to the cell cycle in 267 glioma spheres at the IC_{50} dose (Supplemental Figure 8O). Moreover, exogenous NEK2 or empty vector was overexpressed in 267 glioma spheres and followed by a cytotoxicity assay with CMP3a. The results showed that exogenous NEK2 induced resistance to CMP3a in 267 glioma spheres when compared with the baseline control cells, indicating that CMP3a inhibited tumor proliferation as a result of its inhibition of NEK2 kinase activity (Supplemental Figure 8P).

We then combined CMP3a treatment with radiation in 528 glioma spheres. Western blot analysis indicated that EZH2 expression was increased after radiation and eliminated by NEK2 inhibition with CMP3a (Supplemental Figure 9A). Using cell-growth and sphere-formation assays, we found consistent results between gene silencing and the pharmacological inhibition of NEK2 in glioma spheres. The 528 glioma spheres showed decreased cell proliferation and sphere-formation capability after the combined treatment of CMP3a and radiation (Figure 7J and Supplemental Figure 9B). Next, we combined varying doses of CMP3a with radiation in 528 glioma spheres. The result showed that CMP3a treatment decreased the radioresistance of the 528 glioma spheres in a dose-dependent manner (Supplemental Figure 9C). Furthermore, flow cytometry showed that radiation increased the proportion of apoptotic cells when combined with CMP3a treatment in a dose-dependent manner (Supplemental Figure 9, D and E). To distinguish whether NEK2 inhibition had an additive or synergistic effect with radiation, we applied the Chou-Talalay model to the data (27, 28). The results showed that the combination index (CI) for radiation and CMP3a was less than 1, which indicated that NEK2 inhibition had a synergistic effect with radiation on the 528 glioma spheres (Figure 7K).

Additionally, we used NHAs to assess the safety of CMP3a combined with radiation. Unlike what we observed with GBM cells, the qRT-PCR results showed that NEK2 expression was dramatically decreased after radiation in NHAs (Supplemental Figure 9F), and flow cytometric analysis revealed that CMP3a did not significantly affect the sensitivity of NHA cells to radiation (Supplemental Figure 9G). Altogether, these data suggest that CMP3a decreases radioresistance and abolishes GSC growth by regulating the stability of EZH2 protein (Figure 8).

Discussion

The radioresistance of GBM is a major cause of tumor recurrence and subsequent patient mortality (1). Evidence suggests that GSCs may play a critical role in tumor radiation resistance and subsequent life-threatening recurrence (2). Previously, we identified the serine/threonine kinase MELK as a key regulator of GSC radioresistance via transcriptional regulation of the oncogenic histone H3 methyltransferase EZH2. Our study demonstrated that the short-term inhibition of MELK by the small-molecule inhibitor OTS167, a cancer drug candidate in a phase I study for triple-negative breast cancer, suppressed the downstream signaling driven by EZH2. However, long-term suppression resulted in the reactivation of EZH2 signaling, thereby driving GBM cells to persistently rely on EZH2 dependence for their survival, propagation, and radiation resistance. Through extensive screening using transcriptome and IP techniques, we identified the poorly characterized serine/threonine kinase NEK2 as an alternative mechanism to maintain EZH2 dependence in GSCs. Further characterization based on qRT-PCR data for $CD133^+$ cells in PN glioma sphere cultures and $ALDH1A3^+$ cells in MES glioma sphere cultures demonstrated that NEK2 expression was relatively restricted to the cancer stem cell subpopulation in GBM tumors (25, 29). NEK2 knockdown attenuated GBM cell clonogenicity in vitro and the tumor-initiating ability (tumorigenicity) of GSCs in vivo in 2 patient-derived glioma sphere samples, indicating that NEK2 was required for GSC survival and growth. With regard to the molecular mechanism in GSCs, unlike MELK, NEK2 forms a protein complex with EZH2, thereby phosphorylating and protecting EZH2 from the proteasome-dependent degradation in glioma spheres. Clinically, NEK2 immunoreactivity was negatively linked to GBM patient prognosis, suggesting that NEK2 might be a potential therapeutic target in GBM. As expected, NEK2 expression was markedly elevated in post-radiation recurrent tumors compared with expression levels detected in primary tumors in matched GBM cases, raising the possibility that NEK2 played a role in establishing therapy resistance in GBM. To target

NEK2, we developed a potent and highly selective NEK2 inhibitor through 3 rounds of structural modifications of small molecules using a molecular structure–based drug design. The lead compound, CMP3a, exhibited a set of inhibitory effects on glioma spheres in vitro and GSC-derived mouse GBM tumors in vivo that were consistent with those caused by shRNA-mediated NEK2 knockdown. We are currently in the process of pharmacokinetic and pharmacodynamic analyses with CMP3a to design an early-phase clinical trial for GBM and other NEK2/EZH2-dependent cancers. In addition to these findings, we also found that CMP3a treatment reduced tumor growth in vivo, however, the efficacy of tumor growth inhibition was not as effective as the in vitro knockdown of NEK2. Further studies focusing on the improvement of the bioavailability of CMP3a and the possible development of more efficacious derivatives of CMP3a will need to be performed.

NEK2 encodes a cell-cycle–regulated protein kinase that is localized in the centrosome and required for bipolar spindle formation for mitotic progression (30). NEK2 overexpression has been recognized in various cancers, including breast cancer, lymphoma, testicular seminomas, lung cancer, and colorectal cancer, and it has been shown to correlate with an aggressive phenotype and poor prognoses for these cancers (11, 31–34). A recent study reported that NEK2 silencing by shRNAs reduces tumor cell progression by interference with chromosomal segregation in human breast cancer cell lines in vitro and in fat pad xenograft mouse models, leading to aneuploidy and subsequent cell death (35). Another study indicated that in human lung and colorectal cancer cell lines, NEK2 plays a critical role in the subcellular transfer of β-catenin from the plasma membrane to the cytoplasm and the nucleus, leading to an invasive cellular phenotype in vitro and in vivo (11, 36). Our data indicated that NEK2 expression was elevated in the stem cell fraction in GBM and was essential for GSC stemness in vitro and in vivo. Although OTS167 treatment in GBM mouse models had an initial tumor-suppressive effect, the cellular damage to GSCs appeared to switch their dependence from MELK to NEK2 to retain EZH2 activation. Unlike the MELK signaling mechanism, the regulation of EZH2 by NEK2 was at least partially dependent on the formation of a protein complex that prolonged the half-life of EZH2 by inhibiting its proteasome-dependent degradation in GSCs. These observations highlight what we believe to be a novel function of NEK2 as an essential kinase for GSC stemness and in vivo tumorigenesis in addition to its mitosis-specific functions. Furthermore, we demonstrated that NEK2 overexpression was associated with a poor prognosis in GBM patients and that NEK2 depletion in GSCs increased the radiosensitivity of GSCs, indicating that NEK2 may be a new therapeutic target for radioresistant GBM. Aside from these findings, it is unclear whether NEK2 functions in EZH2 posttranslational regulation by regulating protein modification or perhaps through an alternate, still undetermined mechanism.

Accumulating evidence, along with the contributions from the present study, suggests that EZH2 is a transcriptional silencer in various cancers, including GBM, that protects the cancer stem cells from differentiation and radiation-induced cell death (23, 24, 37–39). Nevertheless, the mechanism of EZH2 protein metabolism in cancers and cancer stem cells remains elusive. A recent study reported that in HEK293T cells, cyclin-dependent kinase 1 (CDK1) mediates EZH2 phosphorylation at Thr345 and Thr487, thereby promoting EZH2 ubiquitination and subsequent degradation by the proteasome in vitro. This CDK1-mediated EZH2 phosphorylation is enriched in cells that are arrested in mitosis compared with S-phase cells (40). Another study reported that treatment of the DNA methylation inhibitor DZNep in 293T cells upregulates the ubiquitin ligase PRAJA1, which degrades EZH2 in vitro (41). Additionally, another study indicated that the SMAD ubiquitination regulatory factor 2 (Smurf2) is an E3 ubiquitin ligase responsible for the polyubiquitination and proteasome-mediated degradation of EZH2 in human mesenchymal stem cells (hMSCs) in vitro and in an intracranial xenograft model (42). These studies provide insights into the mechanism of EZH2 degradation through ubiquitination, mostly in normal somatic cells in vitro. However, there are very limited data on how cancer stem cells regulate the half-life of the EZH2 protein to promote tumor aggressiveness and therapy resistance in GBM. Our data indicated that GSCs used a unique, previously unidentified molecular mechanism to maintain the protein stability of EZH2 via NEK2 as a binding partner to protect EZH2 protein from proteasome-dependent degradation. Interestingly, this signaling axis via the NEK2-EZH2 protein complex was upregulated after cellular damage (e.g., MELK inhibition), although a subset of GBMs might exhibit this upregulation in naive, untreated tumors. Disrupting NEK2-EZH2 interaction in cancer cells had the potential to target their cancer stem cell compartment. This strategy may serve as a new therapeutic approach to treat recurrent tumors and a subgroup of primary tumors. However, whether NEK2-dependent tumor growth depends solely on its interaction with EZH2 or other unidentified signaling molecules such as mitosis-related proteins remains unclear. In addition, the NEK2-mediated protection of EZH2 degradation in GSCs may require some protein modification (e.g., phosphorylation) in the binding domain or elsewhere. Moreover, our results indicated that overexpression of the NEK2 K37R mutant could partially rescue the effects of NEK2 knockdown on glioma cell proliferation, raising the possibility that the interaction between NEK2 and EZH2 might protect EZH2 from degradation by either phosphorylation or physical occupation of the ubiquitination site of EZH2. To answer these questions, further studies are needed to identify the binding structure and the specific phosphorylation site of EZH2.

Methods

Reagents. The following reagents were used in this study: EGF (PeproTech); basic FGF (bFGF) (PeproTech); B27 (Invitrogen, Thermo Fisher Scientific); heparin (Sigma-Aldrich); DMEM-F12 (Gibco, Thermo Fisher Scientific); FBS (Gibco, Thermo Fisher Scientific); Accutase Solution (Sigma-Aldrich); AlamarBlue (Invitrogen, Thermo Fisher Scientific); radio immunoprecipitation assay (RIPA) buffer (Sigma-Aldrich); phosphatase inhibitor cocktail (Sigma-Aldrich); protease inhibitor cocktail (Sigma-Aldrich); Quick Start Bradford Protein Assay (Bio-Rad); BSA (BioLabs); PageRuler Plus Prestained Protein (Thermo Fisher Scientific); iScript Reverse Transcription Supermix (Bio-Rad); Protein A/G Magnetic Beads (Thermo Fisher Scientific); and IP Lysis Buffer (Thermo Fisher Scientific).

Antibodies. The following primary antibodies were used in this study: anti-NEK2 antibody (Abcam; ab117553, mouse, IHC and IP); anti-NEK2 antibody (Thermo Fisher Scientific; PA5-31259, rabbit, ICC); anti-NEK2 antibody (Thermo Fisher Scientific; PA5-15337, rabbit, Western blotting); anti-NEK2 antibody (Abcam; ab55550, mouse,

flow cytometry); anti-EZH2 antibody (Cell Signaling Technology; 4905, rabbit, IP and Western blotting); anti-EZH2 antibody (Thermo Fisher Scientific; MA5-15101, mouse, ICC); anti-H3K27me3 antibody (EMD Millipore; 07-449, rabbit); anti–β-actin antibody (Sigma-Aldrich; A5316, mouse); anti-ubiquitin antibody (Cell Signaling Technology; 3936, mouse); anti–acetylated α-tubulin antibody (Abcam; ab24610, mouse); and anti–phosphorylated serine/threonine antibody (Cell Signaling Technology; 9631, rabbit).

GSC cultures. Glioma sphere cultures from clinical samples were cultured in DMEM/F12 medium containing 2% B27 supplement (% vol), 2.5 mg/ml heparin, 20 ng/ml bFGF, and 20 ng/ml EGF. The bFGF and EGF reagents were added twice a week, and the culture medium was replaced every 10 days. Experiments with neurospheres were performed with lines that were cultured for fewer than 40 passages since their initial establishment. An in vitro limiting dilution neurosphere formation assay and in vitro cell viability assay were performed as previously described (43).

Western blotting. The cell lysates were prepared in RIPA buffer containing 1% protease and 1% phosphatase inhibitor cocktail on ice. The sample protein concentrations were determined using the Bradford method. Equal amounts of protein lysates (10 μg/lane) were fractionated on a NuPAGE Novex 4%–12% Bis-Tris Protein Gel (Invitrogen, Thermo Fisher Scientific) and transferred onto a PVDF membrane (Invitrogen, Thermo Fisher Scientific). Subsequently, the membranes were blocked with 5% skim milk for 1 hour and then treated with the appropriate antibody at 4°C overnight. Protein expression was visualized with an Amersham ECL Western Blot System (GE Healthcare Life Sciences). β-Actin served as a loading control. ImageJ software (NIH) was used to analyze the Western blot results. See complete unedited blots in the supplemental material.

In vivo intracranial xenograft tumor model. Six-week-old female nude mice were used for glioma sphere intracranial xenotransplantation. The glioma sphere suspension (1×10^4 cells for 83 glioma spheres, 1×10^5 cells for 528 glioma spheres, or 1×10^5 cells for 267 glioma spheres in 2 μl PBS) transduced with shNT or shNEK2 lentivirus was injected into the brains of the nude mice as previously described (25, 29). Six mice were used for each group. When neuropathological symptoms developed, the mice were sacrificed and perfused with ice-cold PBS and 4% (wt/vol) paraformaldehyde (PFA). Then, the mice brains were dissected and fixed in 4% PFA for 24 hours, transferred to 10% formalin, and sectioned. Mice were administered the drug via a tail vein injection.

Further details on the materials and methods used can be found in the Supplemental Methods.

Statistical analysis. All data are expressed as the mean ± SD. The number of replicates for each experiment is stated in the figure legends. Statistical differences between 2 groups were evaluated using a 2-tailed *t* test. Multiple group comparisons were performed using a 1-way ANOVA followed by Dunnett's post-hoc test. The in vitro clonogenicity assays were analyzed using extreme limiting dilution analysis (ELDA). The significance of a Kaplan-Meier survival plot was determined by log-rank analysis. Statistical analysis was performed using GraphPad Prism 6 and SPSS 19.0 software. A *P* value of less than 0.05 was considered statistically significant.

Study approval. This study was conducted under protocols approved by the IRBs and IACUCs of UCLA, MD Anderson Cancer Center (MDA), the University of Alabama at Birmingham (UAB), and The Ohio State University (OSU).

Author contributions

JW, MSP, and YJS performed the experiments. JW, PC, MSP, ZZ, MM, DC, YL, DHN, and IN analyzed the data. JW, PC, MW, AM, SHK, HY, HIK, and IN wrote the manuscript. BF, WH, and HL designed, synthesized, and screened the NEK2 inhibitors and performed the in vitro KINOMEscan and PK analysis. shRNAs for NEK2 were provided by VG. Patient samples from Department of Neurosurgery, The First Affiliated Hospital of Xi'an Jiaotong University were collected and analyzed by JW, WX, and MW.

Acknowledgments

We thank all the members of the Nakano laboratory for constructive discussion of this study. This study was supported by the following NIH grants: P01CA163205 (to IN); R01NS083767 (to IN); R21CA175875 (to IN); R01NS087913 (to IN); R01CA183991 (to IN); 3T32GM008804-10S1 (to HL); and 5T32GM008804-10 (to HL). JW was supported by The First Affiliated Hospital of Xi'an Jiaotong University and the China Scholar Council. MP was supported by the Russian Foundation for Basic Research grant 16-04-01209 and by the Scholarship of the President of the Russian Federation. Additional supports were from the grant of Korea Health Technology R&D Project through the Korea Health Industry Development Institute (KHIDI), funded by the Ministry of Health & Welfare, Republic of Korea (HI14C3418).

Address correspondence to: Ichiro Nakano, Department of Neurosurgery, Comprehensive Cancer Center, University of Alabama at Birmingham, WTI 401, 1824 6th Avenue South, Birmingham, Alabama 35233, USA. Phone: 205.996.0071; Email: inakano@uabmc.edu. Or to: Maode Wang, Department of Neurosurgery, The First Affiliated Hospital of Xi'an Jiaotong University, 277 Yanta West Road, Xi'an, Shaanxi, China 710061. Phone: 86.029.85323989; Email: maodewang@163.com.

1. Linz U. Commentary on Effects of radiotherapy with concomitant and adjuvant temozolomide versus radiotherapy alone on survival in glioblastoma in a randomised phase III study: 5-year analysis of the EORTC-NCIC trial (Lancet Oncol. 2009;10:459-466). *Cancer*. 2010;116(8):1844–1846.
2. Sundar SJ, Hsieh JK, Manjila S, Lathia JD, Sloan A. The role of cancer stem cells in glioblastoma. *Neurosurg Focus*. 2014;37(6):E6.
3. Lawrence YR, et al. Improving prognosis of glioblastoma in the 21st century: who has benefited most? *Cancer*. 2012;118(17):4228–4234.
4. Stupp R, et al. Radiotherapy plus concomitant and adjuvant temozolomide for glioblastoma. *N Engl J Med*. 2005;352(10):987–996.
5. Hingtgen S, et al. Real-time multi-modality imaging of glioblastoma tumor resection and recurrence. *J Neurooncol*. 2013;111(2):153–161.
6. Yang HW, Xing H, Johnson MD. A major role for microRNAs in glioblastoma cancer stem-like cells. *Arch Pharm Res*. 2015;38(3):423–434.
7. Oike T, et al. Radiotherapy plus concomitant adjuvant temozolomide for glioblastoma: Japanese mono-institutional results. *PLoS One*. 2013;8(11):e78943.
8. Network TC. Corrigendum: Comprehensive genomic characterization defines human glioblastoma genes and core pathways. *Nature*. 2013;494(7438):506.
9. Nickel GC, et al. Characterizing mutational heterogeneity in a glioblastoma patient with double recurrence. *PLoS One*. 2012;7(4):e35262.
10. Lee J, Gollahon L. Nek2-targeted ASO or siRNA pretreatment enhances anticancer drug sensitivity in triple-negative breast cancer cells. *Int J*

Oncol. 2013;42(3):839–847.
11. Neal CP, et al. Overexpression of the Nek2 kinase in colorectal cancer correlates with beta-catenin relocalization and shortened cancer-specific survival. *J Surg Oncol*. 2014;110(7):828–838.
12. Bahe S, Stierhof YD, Wilkinson CJ, Leiss F, Nigg EA. Rootletin forms centriole-associated filaments and functions in centrosome cohesion. *J Cell Biol*. 2005;171(1):27–33.
13. Mayor T, Hacker U, Stierhof YD, Nigg EA. The mechanism regulating the dissociation of the centrosomal protein C-Nap1 from mitotic spindle poles. *J Cell Sci*. 2002;115(Pt 16):3275–3284.
14. Zhou W, et al. NEK2 induces drug resistance mainly through activation of efflux drug pumps and is associated with poor prognosis in myeloma and other cancers. *Cancer Cell*. 2013;23(1):48–62.
15. Hayward DG, Fry AM. Nek2 kinase in chromosome instability and cancer. *Cancer Lett*. 2006;237(2):155–166.
16. Takahashi Y, et al. Up-regulation of NEK2 by microRNA-128 methylation is associated with poor prognosis in colorectal cancer. *Ann Surg Oncol*. 2014;21(1):205–212.
17. Liu X, Gao Y, Lu Y, Zhang J, Li L, Yin F. Upregulation of NEK2 is associated with drug resistance in ovarian cancer. *Oncol Rep*. 2014;31(2):745–754.
18. Wei R, Ngo B, Wu G, Lee WH. Phosphorylation of the Ndc80 complex protein, HEC1, by Nek2 kinase modulates chromosome alignment and signaling of the spindle assembly checkpoint. *Mol Biol Cell*. 2011;22(19):3584–3594.
19. Margueron R, Reinberg D. The Polycomb complex PRC2 and its mark in life. *Nature*. 2011;469(7330):343–349.
20. Cao R, et al. Role of histone H3 lysine 27 methylation in Polycomb-group silencing. *Science*. 2002;298(5595):1039–1043.
21. Simon JA, Lange CA. Roles of the EZH2 histone methyltransferase in cancer epigenetics. *Mutat Res*. 2008;647(1-2):21–29.
22. Lee J, et al. Epigenetic-mediated dysfunction of the bone morphogenetic protein pathway inhibits differentiation of glioblastoma-initiating cells. *Cancer Cell*. 2008;13(1):69–80.
23. Kim E, et al. Phosphorylation of EZH2 activates STAT3 signaling via STAT3 methylation and promotes tumorigenicity of glioblastoma stem-like cells. *Cancer Cell*. 2013;23(6):839–852.
24. Kim SH, et al. EZH2 protects glioma stem cells from radiation-induced cell death in a MELK/FOXM1-dependent manner. *Stem Cell Reports*. 2015;4(2):226–238.
25. Mao P, et al. Mesenchymal glioma stem cells are maintained by activated glycolytic metabolism involving aldehyde dehydrogenase 1A3. *Proc Natl Acad Sci USA*. 2013;110(21):8644–8649.
26. Rellos P, et al. Structure and regulation of the human Nek2 centrosomal kinase. *J Biol Chem*. 2007;282(9):6833–6842.
27. Chou TC. Drug combination studies and their synergy quantification using the Chou-Talalay method. *Cancer Res*. 2010;70(2):440–446.
28. Ashton JC. Drug combination studies and their synergy quantification using the Chou-Talalay method--letter. *Cancer Res*. 2015;75(11):2400.
29. Cheng P, et al. Kinome-wide shRNA screen identifies the receptor tyrosine kinase AXL as a key regulator for mesenchymal glioblastoma stem-like cells. *Stem Cell Reports*. 2015;4(5):899–913.
30. Bayliss R, Fry A, Haq T, Yeoh S. On the molecular mechanisms of mitotic kinase activation. *Open Biol*. 2012;2(11):120136.
31. Hayward DG, Clarke RB, Faragher AJ, Pillai MR, Hagan IM, Fry AM. The centrosomal kinase Nek2 displays elevated levels of protein expression in human breast cancer. *Cancer Res*. 2004;64(20):7370–7376.
32. Andréasson U, et al. Identification of molecular targets associated with transformed diffuse large B cell lymphoma using highly purified tumor cells. *Am J Hematol*. 2009;84(12):803–808.
33. Barbagallo F, et al. Increased expression and nuclear localization of the centrosomal kinase Nek2 in human testicular seminomas. *J Pathol*. 2009;217(3):431–441.
34. Zhong X, Guan X, Liu W, Zhang L. Aberrant expression of NEK2 and its clinical significance in non-small cell lung cancer. *Oncol Lett*. 2014;8(4):1470–1476.
35. Cappello P, et al. Role of Nek2 on centrosome duplication and aneuploidy in breast cancer cells. *Oncogene*. 2014;33(18):2375–2384.
36. Das TK, et al. Centrosomal kinase Nek2 cooperates with oncogenic pathways to promote metastasis. *Oncogenesis*. 2013;2:e69.
37. Hu S, et al. Overexpression of EZH2 contributes to acquired cisplatin resistance in ovarian cancer cells in vitro and in vivo. *Cancer Biol Ther*. 2010;10(8):788–795.
38. Zhou W, Wang J, Man WY, Zhang QW, Xu WG. siRNA silencing EZH2 reverses cisplatin-resistance of human non-small cell lung and gastric cancer cells. *Asian Pac J Cancer Prev*. 2015;16(6):2425–2430.
39. Gibaja V, et al. Development of secondary mutations in wild-type and mutant EZH2 alleles cooperates to confer resistance to EZH2 inhibitors. *Oncogene*. 2016;35(5):558–566.
40. Wu SC, Zhang Y. Cyclin-dependent kinase 1 (CDK1)-mediated phosphorylation of enhancer of zeste 2 (Ezh2) regulates its stability. *J Biol Chem*. 2011;286(32):28511–28519.
41. Zoabi M, Sadeh R, de Bie P, Marquez VE, Ciechanover A. PRAJA1 is a ubiquitin ligase for the polycomb repressive complex 2 proteins. *Biochem Biophys Res Commun*. 2011;408(3):393–398.
42. Yu YL, et al. Smurf2-mediated degradation of EZH2 enhances neuron differentiation and improves functional recovery after ischaemic stroke. *EMBO Mol Med*. 2013;5(4):531–547.
43. Cheng P, et al. FOXD1-ALDH1A3 Signaling Is a Determinant for the Self-Renewal and Tumorigenicity of Mesenchymal Glioma Stem Cells. *Cancer Res*. 2016;76(24):7219–7230.